Published for SISSA by Springer

Received: June 8, 2018
Revised: August 28, 2019
Accepted: October 8, 2019
Published: October 23, 2019

Prospects for disentangling long- and short-distance effects in the decays $B \to K^* \mu^+ \mu^-$

Marcin Chrzaszcz,[a,b,c] **Andrea Mauri,**[b] **Nicola Serra,**[b] **Rafael Silva Coutinho**[b] **and Danny van Dyk**[b,d]

[a] *European Organization for Nuclear Research (CERN), Geneva, Switzerland*
[b] *Universität Zürich, Physik Institut, Winterthurer Strasse 190, 8057 Zürich, Switzerland*
[c] *Henryk Niewodniczanski Institute of Nuclear Physics Polish Academy of Sciences, Kraków, Poland*
[d] *Physik Department, Technische Universität München, James-Franck-Straße 1, 85748 Garching, Germany*

E-mail: marcin.chrzaszcz@cern.ch, a.mauri@cern.ch, Nicola.Serra@cern.ch, rafael.silva.coutinho@cern.ch, danny.van.dyk@gmail.com

Abstract: Theory uncertainties on non-local hadronic effects limit the New Physics discovery potential of the rare decays $B \to K^* \mu^+ \mu^-$. We investigate prospects to disentangle New Physics effects in the short-distance coefficients from these effects. Our approach makes use of an event-by-event amplitude analysis, and relies on a particular parametrisation of the non-local contributions. We find that non-standard effects in the short-distance coefficients can be successfully disentangled from non-local hadronic effects. The impact of the truncation on the parametrisation of non-local contributions to the Wilson coefficients are for the first time systematically examined and prospects for their precise determination are discussed. Theoretical inputs on the non-local matrix elements beyond the physically-accessible phase space are crucial to stabilise the determination of Wilson coefficients, while we find that physical observables are unaffected by these uncertainties. Compared to other methods, our approach provides for a more precise extraction of the angular observables from data.

Keywords: B physics, Beyond Standard Model, Flavour Changing Neutral Currents, Hadron-Hadron scattering (experiments)

ArXiv ePrint: 1805.06378

https://doi.org/10.1007/JHEP10(2019)236

JHEP10(2019)236

Contents

JHEP10(2019)236

1 Introduction

The sensitivity of the decay $B \to K^*\mu^+\mu^-$ to effects of beyond the Standard Model (SM) physics is well known (see e.g. [1] for a review). Consequently, this decay is one of the standard candles in indirect searches for New Physics (NP) effects. A recent analysis of this decay by the LHCb collaboration has first established [2] the so-called P_5' [3] "anomaly", i.e. a deviation in measurements of that observable from the SM predictions by $\sim 3\sigma$. Subsequent analyses by both LHCb [4] and Belle [5] further increased the tension between the SM predictions and the data. Non-standard measurements of the Lepton-Flavour-Universality (LFU) ratios in $b \to s\ell\ell$ processes — such as of R_K and R_{K^*} [6] by LHCb [7, 8] — suggest that a NP explanation of the P_5' anomaly could simultaneously be LFU violating.

In their attempts to understand the anomalies, many phenomenological studies of this decay strive to model-independently constrain the effects of New Physics. This is usually achieved within the framework of an effective field theory. Within the latter, a subset of

the Wilson coefficients C_i for the basis of dimension-six operators O_i are fitted from data. For the purpose of this letter, we use the effective weak Lagrangian [9],

$$\mathcal{L}^{\text{eff}} = \frac{4G_F}{\sqrt{2}} V_{tb}V_{ts}^* \Big\{ [C_1 O_1^c + C_2 O_2^c] + \frac{\alpha_e}{4\pi} [C_7 O_7 + C_9 O_9 + C_{10} O_{10}] \Big\} + \mathcal{O}\left(\frac{V_{ub}V_{us}^*}{V_{tb}V_{ts}^*}, C_{3,\dots,6}, \alpha_s C_8 \right) , \tag{1.1}$$

with the current-current operators

$$O_1^c = \left[\bar{s}\gamma^\mu P_L T^A c\right] \left[\bar{c}\gamma_\mu P_L T^A b\right] , \qquad O_2^c = \left[\bar{s}\gamma^\mu P_L c\right] \left[\bar{c}\gamma_\mu P_L b\right] , \tag{1.2}$$

and radiative/semileptonic operators

$$O_7 = \frac{m_b}{e} \left[\bar{s}\sigma^{\mu\nu} P_R b\right] F_{\mu\nu} , \quad O_9 = \left[\bar{s}\gamma^\mu P_L b\right] \left[\bar{\ell}\gamma_\mu \ell\right] , \quad O_{10} = \left[\bar{s}\gamma^\mu P_L b\right] \left[\bar{\ell}\gamma_\mu \gamma_5 \ell\right] . \tag{1.3}$$

Our conventions are the same as the ones of ref. [10], which we follow closely. The idea to extract the Wilson coefficients C_i was first discussed in ref. [11]. The extraction is predicated on setting the renormalisation scale of the matrix elements. We adhere to the common choice[1] of $\mu = 4.2\,\text{GeV} \simeq \overline{m}_b(\overline{m}_b)$. For our purpose, we will focus on the extraction of C_9 and C_{10}. The latter does not mix with other coefficients under change of the renormalisation scale up to electroweak corrections. In the renormalisation of C_9 at scales $\mu \sim m_b$ on the other hand, the numerically leading effects is mostly additive, see e.g. [12]:

$$C_9(\mu) - C_9(m_b) \sim \sum_{i=1}^{2} C_i(m_b)\, \gamma_{i9}^{(0)} \log \frac{m_b}{\mu} + \text{higher orders in } \alpha_s \text{ and } C_{3,\dots,6}. \tag{1.4}$$

In the above, $\gamma_{ij}^{(0)}$ denotes the leading-order term in the anomalous mass dimension with operator indices i and j.

A detriment to extracting the C_i, for $i = 7, 9, 10$ from data is our lack of knowledge of the hadronic matrix elements of the operators O_i. For local interactions, these matrix elements are expressed in terms of hadronic form factors. The latter can be accessed either from first principles through Lattice QCD simulations, or from quark-hadron-duality arguments through QCD Light-Cone Sum Rules (LCSRs). The matrix elements of non-local operators involving insertions of $O_{1,2}$, however, turn out to be more difficult to determine, and have been the focus of much attention over the last two decades. Presently, the largest systematic uncertainty in determinations of the Wilson Coefficient C_9 arises from our lack of understanding of the non-local hadronic matrix elements

$$\mathcal{H}^\mu(q,k) \equiv \int d^4x\, e^{iqx} \langle K^*(k)|\, \mathcal{T}\{J^\mu_{\text{e.m.}}(x), \mathcal{O}_{bscc}(0)\}\, |\bar{B}(q+k)\rangle \tag{1.5}$$

where $J_{\text{e.m.}}$ denotes the electromagnetic current, and

$$\mathcal{O}_{bscc} \equiv C_1 O_1^c + C_2 O_2^c \tag{1.6}$$

[1] While this is a common choice, we emphasize that for applications of our approach to data the uncertainty of the extraction of C_9 should be estimated by repeated determinations of C_9 at different scales.

JHEP10(2019)236

represents the four quark operator involving two charm quark fields. In the above k denotes the four-momentum of the final-state hadron, and q describes the momentum transfer to the virtual photon. It is convenient to decompose $\mathcal{H}^\mu$ into scalar-valued Lorentz-invariant quantities $\mathcal{H}_\lambda(q^2)$ as in [10]. Here $\lambda = 0, \perp, \parallel$ denotes the polarisation state of the dilepton system.

The objects $\mathcal{H}_\lambda$ can be accessed in the limit of large kaon energy in the B rest frame, or equivalently for[2] $m_b \Lambda_{\text{hadr.}} \lesssim q^2 \lesssim$ a few $\text{GeV}^2 \ll m_b^2$ [13, 14]. This QCD Factorisation (QCDF) approach has inspired a larger number of phenomenological analyses. However, all of these studies treat the off-shell contributions from the charm pair as perturbative, even though this is likely to receive substantial corrections from soft-gluon emissions [15] off the charm loop, even for the region $1\,\text{GeV}^2 \leq q^2 \leq 6\,\text{GeV}^2$ that is usually used for phenomenological studies. An alternative to a theoretical determination of $\mathcal{H}$ are data-driven analyses[3] [16–20]. Some of these analyses show promise in fitting a resonance model to the q^2 spectrum. Others determine the non-local contributions below the J/ψ from data. Both approached therefore give access to *model-dependent* determinations of the WC C_9. In addition, information on the model parameters are only available a-posteriori, which precludes genuine SM predictions of the observables.

Both drawbacks, the perturbative treatment of the charm quarks at timelike q^2 and the model assumptions in the parametrisation of the q^2 spectrum have been recently overcome and reduced, respectively, through a parametrisation that is valid for $-7\,\text{GeV}^2 \lesssim q^2 \leq M^2_{\psi(2S)}$ [10]. In that study, pseudo observables based on the theoretical predictions are generated at $q^2 < 0$, for which one expects better convergence of the Light-Cone OPE [15]. In addition, the residues of the scalar valued correlators $\mathcal{H}_\lambda(q^2)$ can be constrained from experimental results on the branching ratios and angular distribution of the hadronic decays $B \to \psi_n K^*$, where $\psi_n = J/\psi, \psi(2S)$. Last but not least, expressing the ratio of the $\mathcal{H}_\lambda$ over their corresponding (local) form factors $\mathcal{F}_\lambda$ in combination with an expansion in the variable z ensures the correct analytic behaviour. Since we follow the results of reference [10] closely, the parametrisation used for the correlators $\mathcal{H}_\lambda(q^2)$, which is briefly summarised in appendix A, does not reproduce the physical light-hadron cut starting at $q^2 = 4M_\pi^2$. However, it has been argued that this cut is suppressed [10], and we will discuss — in parts — its numerical impact and the possible model bias that the lack of the cut introduces in section 3.

Given this recent progress on the non-local matrix elements we now aim to study the possibility of applying the z expansion to future experimental analyses: first, we want to establish to which extent information concerning the non-local matrix elements can be inferred from experimental data of the semileptonic decay. In order to maximise the sensitivity to the parameters, we will focus on an extended unbinned analysis of the data; an extension of our study to unbinned analyses that include the $K\pi$ S-wave background is summarised in appendix B. Second, we investigate the convergency of the series expansion

[2] The lower boundry on the q^2 range arises from a breakdown of QCDF for the longitudinal amplitude in this phase space region; see [13].

[3] These analyses apply also to the decay $B \to K\mu^+\mu^-$, which has a reduced complexity compared to the decay $B \to K^*\mu^+\mu^-$ discussed in this letter.

JHEP10(2019)236

at different order of z and what is the residual model-bias introduced by truncations. Finally, we want to establish the smallest amount of theoretical inputs necessary to find evidence for new phenomena in quark-flavour physics in a single $b \to s\ell\ell$ process and through a single measurement.

2 Preliminaries

Assuming on-shell K^* dominance, the decay $B \to K^*(\to K\pi)\mu^+\mu^-$ involves four kinematic variables: the dimuon mass square q^2, as well as two helicity angles within the $\mu^+\mu^-$ and $K\pi$ decay planes, respectively, and the azimuthal angle between the planes (see [21, 22] and subsequent publications). The Probability Density Function (PDF) for this decay gives rise to a larger number of angular observables, which can be used to extract information on the short-distance physics. Here, we do not use these angular observables directly, but rather use the angular information of the signal PDF for $B \to K^*(\to K\pi)\mu^+\mu^-$ decays in its entirety.

We work with two signal PDFs: pDF_1 and PDF_2, defined as

$$\text{PDF}_i \equiv \frac{1}{\Gamma_i}\frac{\mathrm{d}^4\Gamma}{\mathrm{d}q^2\,\mathrm{d}^3\Omega}\,, \qquad \text{with} \quad \Gamma_i \equiv \int_{q^2\in Q_i} \mathrm{d}q^2\,\frac{\mathrm{d}\Gamma}{\mathrm{d}q^2}\,. \tag{2.1}$$

Here the four-differential rate is a sesquilinear form of the set of transversity amplitudes $A_\lambda(q^2)$, with polarisation states $\lambda = \perp, \parallel, 0, t$ [9]. For later discussion, it is instrumental to understand that the amplitudes with $\lambda = \perp, \parallel, 0$ can (in the SM) be written as [10]

$$\begin{aligned}\mathcal{A}_\lambda^{L,R} =& \mathcal{N}_\lambda \left\{(C_9 \mp C_{10})\mathcal{F}_\lambda(q^2) + \frac{2m_b M_B}{q^2}\left[C_7\mathcal{F}_\lambda^T(q^2) - 16\pi^2\frac{M_B}{m_b}\mathcal{H}_\lambda(q^2)\right]\right\} \\ &+ \mathcal{O}\left(C_{3,\ldots,6,}, C_8, \left|V_{ub}V_{us}\right|\right)\,.\end{aligned} \tag{2.2}$$

In the above, the functions $\mathcal{F}_\lambda^{(T)}(q^2)$ stand for (linear combinations) of local form factors (FF), while the non-local matrix elements $\mathcal{H}_\lambda(q^2)$ have been introduced in section 1. The effects of O_8, while not suppressed by a small Wilson coefficient, are nevertheless small due to the size of the hadronic matrix elements [23].

The PDFs describe the combined q^2 and full-angular distribution of the decay in two kinematic regions:

$$\begin{aligned} Q_1: &\quad 1.1\,\text{GeV}^2 \le q^2 \le 9.0\,\text{GeV}^2\,, \\ Q_2: &\quad 10.0\,\text{GeV}^2 \le q^2 \le 13.0\,\text{GeV}^2\,. \end{aligned} \tag{2.3}$$

Note that we impose no constraints on the angular support in either of the PDFs. For a definition of $\mathrm{d}^4\Gamma/(\mathrm{d}q^2\,\mathrm{d}^3\Omega)$ we refer to [24, 25] and references therein.

We produce toy ensembles using the central values of the input parameters $\{\alpha_j\} \equiv \{\alpha_k^{(\lambda)}\} \cup \{\alpha_l^{(F)}\} \cup \{\alpha_m^{(\text{CKM})}\}$, where the individual parameter sets are:

- the correlator parameters $\{\alpha_k^{(\lambda)}\}$ for each polarisation $\lambda = \perp, \parallel, 0$ as specified in [10], corresponding to a nominal truncation at z^2;

	LHCb Run I	LHCb Run II	LHCb Upgrade [50 fb^{-1}]	Belle II [50 ab^{-1}]
N	1850	6,900	62,000	6,100

Table 1. Number of produced pseudo events per toy experiment.

- the form factor parameters $\{\alpha_l^{(F)}\}$ for form factors $F = V, A_{0,\ldots,2}, T_{1,\ldots,3}$ as determined from a combined fit to LCSR and lattice QCD results in [26], but with twice the stated uncertainty;

- and the CKM Wolfenstein parameters $\{\alpha_m^{(\mathrm{CKM})}\} \equiv \{\lambda, A, \bar{\rho}, \bar{\eta}\}$, as obtained from a tree-level analysis of the unitarity triangle [27].

Toy ensembles are either labelled as "SM", in which case we fix all Wilson Coefficients (WCs) to their SM values; or "Benchmark Point" ("BMP"), in which case the WC C_9 is shifted by -1 from its SM value. Each toy ensemble consists of $N \equiv N_1 + N_2$ toy events, which are drawn from the combined log-PDF $\ln \mathrm{PDF} \equiv \ln \mathrm{PDF}_1 + \ln \mathrm{PDF}_2$ of the aforementioned two q^2 regions (see eq. (2.3)). The total number of events N is varied to explore the sensitivity for present and future experiments.

In all cases under study, we maximise the total log-likelihood $\ln \mathcal{L}_{\mathrm{tot}} \equiv \ln \mathcal{L}_1 + \ln \mathcal{L}_2 + \ln \mathcal{L}_{\mathcal{B}}$ with respect to the nuisance parameters $\{\alpha_j\}$ and additionally — for New Physics fits — the WCs C_9 and (in some cases) C_{10}. Here $\mathcal{L}_{1,2}$ are unbinned likelihoods of N_i toy events $x_{n,i} \sim \mathrm{PDF}_i$,

$$\ln \mathcal{L}_i \left(\{\alpha_j\}\right) \equiv \sum_n^{N_i} \ln \mathrm{PDF}_i(x_{n,i} \,|\, \{\alpha_j\}) \,. \tag{2.4}$$

The last term, $\mathcal{L}_{\mathcal{B}}$, incorporates two Poissonian terms for the integrated branching ratios of the decay in the kinematics regions Q_1 and Q_2, respectively. These terms take into account the observed signal rate in a given region of interest and provide complementary information with respect to the normalised four-dimensional PDFs of eq. (2.1).

We then perform a series of frequentist fits to determine the viability of the approach, and to determine uncertainty intervals for the various parameters. In our nominal fits up to z^2, we float the full set of 39 nuisance parameters $\{\alpha_j\}$, with Gaussian constraints as described above. Exception to this are marked appropriately in the text. All quoted 68% confidence level intervals are determined from profile likelihoods. For our studies we are using the same setup as in [10], however independently implemented and cross-checked against the EOS software [28].

The LHCb experiment has already observed 969 and 330 $B^0 \to K^{*0}\mu^+\mu^-$ events in the bins $1.1\,\mathrm{GeV}^2 \leq q^2 \leq 8.0\,\mathrm{GeV}^2$ and $11.0\,\mathrm{GeV}^2 \leq q^2 \leq 12.5\,\mathrm{GeV}^2$, respectively [4]. Extrapolating in q^2 to the larger bin widths as defined in eq. (2.3), we fix $N_{\text{LHCb-Run I}} \equiv 1850$. In the same fashion we obtain $N_{\text{Belle}} = 56$. In order to study the sensitivities for future data sets, we extrapolate the number of events by scaling the luminosities and $b\bar{b}$ production cross section $\sigma_{b\bar{b}}(s)$, where $\sqrt{s}$ denotes the designed centre-of-mass energy of the b-quark pair and for the LHCb experiment we use $\sigma_{b\bar{b}} \propto \sqrt{s}$. The exact numbers of simulated events for each experiment are listed in table 1.

JHEP10(2019)236

Modelling of both the detector resolution or detection efficiency is hardly possible without access to (non-public) information of the current B physics experiments Belle (II) and LHCb. We therefore assume perfect resolution and efficiency in our studies herefrom out — unless otherwise stated. As a consequence, all of our following results should be understood as maximal sensitivity of any future experimental analysis following our suggestions.

Note that we do not study the hadronic uncertainties in the context of free floating parameters for further WCs[4] beside C_9 and C_{10}, since the remaining WCs of semileptonic operators can be disentangled from C_9 as various global analyses of $b \to s\ell\ell$ processes have shown; see e.g. [29–33]. In addition, the WCs C_7 and $C_{7'}$ are strongly constrained by radiative B decays [34]. Moreover, the hadronic non-local effects can always be attributed to q^2-dependent shifts of the WCs C_9 and $C_{9'}$ (the chirality-flipped counterpart to C_9). Sizeable shifts to $C_{9'}$ require NP contributions of non-SM chirality in the operators $O^{(c)}_{1'(2')}$, which are disfavoured by global analyses; see also [35] for a related discussion in the presence of (pseudo)scalar four-quark operators. While the restriction to a sub-set of operators could introduce some model dependency, we are convinced that it suffices to demonstrate the separability of hadronic and NP contributions to C_9 as we set out to do in this article.

3 Initial study

Our main questions concerning the prospects of future analyses pertain to disentangling the hadronic effects of the hadronic correlators from NP effects in the Wilson coefficient C_9.

These questions are:

A Can the parameters $\{\alpha_k^{(\lambda)}\}$ describing the non-local charm contributions be extracted from semileptonic data only (i.e., without theory input through Gaussian constraints)?

B The present theory results for the parameters $\{\alpha_k^{(\lambda)}\}$ of the hadronic correlator assume stable charmonia J/ψ and $\psi(2S)$, i.e., vanishing width for these states. Does neglecting their finite widths introduce a numerically relevant systematic bias in the extraction of the nuisance parameters?

C What residual model-bias is introduced by cutting off the series expansion of the $\mathcal{H}_\lambda(q^2)$ at the power of z^2?

3.1 Determining the $\alpha^{(\lambda)}_{k\leq 2}$ parameters without theory constraints

Prior theoretical knowledge can be used in the fits through Gaussian constraints on the nuisance parameters $\alpha_k^{(\lambda)}$ describing the non-local correlator. However, these constraints can only be produced for parametrisations with a truncation at z^2 [10]. Here we investigate if, in principle, one could abstain from using Gaussian constraints on these parameters, and instead determine them only from data of the semileptonic decay.

In order to answer this question, we perform our analyses in two ways. For our first analysis, we use the constraints provided in [10], which are based on theory calculations in

[4] We thank Sébastien Descotes-Genon for raising this question in private communications.

JHEP10(2019)236

the negative q^2 region, as well as experimental measurements of the angular distributions of the decays $B \to K^* J/\psi$ and $B \to K^* \psi(2S)$. These constraints are included in form of a multivariate Gaussian distribution with correlation information taken into account. Our second analysis does not use either source of information as a constraint on the parameters $\{\alpha_k^{(\lambda)}\}$, and floats them instead within the range $\alpha_k^{(\lambda)} \in [-10^{-2}, +10^{-2}]$.

A series of 500 toy data sets have been produced with the BMP scenario, and then fitted with and without usage of the constraints. From our toy analyses we conclude the following:

1. The analysis with Gaussian constraints on the parameters $\{\alpha_k^{(\lambda)}\}$ is able to extract additional information on the hadronic correlators from the fit, i.e., the obtained uncertainties are smaller than the corresponding Gaussian constraints. The uncertainties on the hadronic parameters scale by a factor between 0.5 and 0.8 for the expected statistics of the LHCb Run II.

2. When removing the constraints, we find that the fit still converges, and that we are able to disentangle hadronic effects from NP in C_9. Our estimator for C_9 is unbiased for a large number of events $\sim$ 30k. For the expected statistics of the LHCb Run II the uncertainties obtained from the fit on the parameters $\{\alpha_k^{(\lambda)}\}$ are found to be comparable to the ones from the prior predictions [10].

3.2 Finite-width effects

The constraints for the parameters $\{\alpha_k^{(\lambda)}\}$ are based [10] on theoretical results (at negative q^2) and the residues of the $\psi = \{J/\psi, \psi(2S)\}$ poles of the correlation functions $\mathcal{H}_\lambda(q^2)$ in the complex q^2 plane. Information on the residues can be obtained from experimental results for the angular distribution of the decays $B \to K^*(\to K\pi)\psi(\to \mu^+\mu^-)$ in small mass windows around the respective ψ masses. In reference [10], the narrow charmonia have been assumed to be stable to simplify the discussion. As a consequence, the poles of the proposed parametrisation are located on the real q^2 axis. However, the physical poles are shifted below the real axis by finite-width effects. Moreover, the shift is directly connected to the q^2 shape of the resonances.

In order to study possible bias introduced by neglecting the width of the narrow charmonia, we study an ensemble of 1k toy analyses corresponding to $N_{\text{LHCb Upgrade}} = 62\text{k}$ events each. We produce the toy events for each fit by using the SM scenario. For each toy analysis we perform two fits to the toy data: one with the nominal PDF, and one for which we modify the PDF such that the poles corresponding to the two narrow charmonium states are shifted below the real q^2-axis by $iM_\psi\Gamma_\psi$. Note that since this shift is not q^2 dependent, the induced imaginary part does not vanish for $q^2 < 4M_\pi^2$. Consequently, our fit PDF does not respect unitarity. However, since it is only used to model possible fit bias at $q^2 \geq 1\,\text{GeV}^2 \gg 4M_\pi^2$, this does not pose a problem here.[5]

We carry out both fits, with the nominal and the modified PDF *without the usage of any Gaussian constraints on the parameters* $\{\alpha_k^{(\lambda)}\}$. We find that the results of the

[5]Effects of non-vanishing width very close to or on the J/ψ, $\psi(2S)$ resonances, as well as for $q^2 \leq 0$ are tightly related to the theory prior and therefore not studied here.

JHEP10(2019)236

fits to toys with and without the width effects are indistinguishable even for an ensemble corresponding to the LHCb Upgrade. As such, the bias introduced by neglecting the finite width *in the semileptonic regions* Q_1 and Q_2 will not play a relevant role for any of the upcoming data sets.

3.3 Model bias of and sensitivity to higher orders in z

In the analysis [10] the truncation order was chosen as $K = 2$, in order to ensure that a-priori predictions (i.e., genuine SM predictions without using $B \to K^*\mu^+\mu^-$ data) can be made. In the applications discussed here we are not bound to using the priors presented in [10] as Gaussian constraints; see section 3.1. Thus, we can explore the sensitivity to coefficients that enter with z^3 or even higher powers in z. Including these in the experimental analysis has the potential to reduce the model-dependence of the results on C_9 due to the z truncation.

We choose to probe the sensitivity to coefficients of order z^3 as follows: we first produce 4k toy analyses with data sets corresponding to the LHCb Run II luminosity. For each study, the pseudo events follow from the BMP scenario. In addition, we introduce the coefficients $\{\alpha_3^{(\lambda)}\}$ for the higher order terms in the correlators $\mathcal{H}_\lambda(q^2)$. We produce toys for $\alpha_3^{(\lambda)} = 0 \;\forall\; \lambda = \perp, \|, 0$. However, in the fit we let the $\{\alpha_3^{(\lambda)}\}$ float freely and determine their 68% CL intervals. We find

$$\sigma\left(\mathrm{Re}\,\alpha_3^{(\lambda)}\right) = 5 \cdot 10^{-3}\,, \quad \sigma\left(\mathrm{Im}\,\alpha_3^{(\lambda)}\right) = 6 \cdot 10^{-3}\,. \tag{3.1}$$

Consequently, we find no sensitivity to coefficients which are smaller in magnitude than $5 \cdot 10^{-3}$.

We also investigate if the value of C_9 obtained from a fit to order z^3 is fully compatible with the fit to order z^2. Our analysis yields

$$C_9\big|_{z^3\text{ fit}} - C_9\big|_{z^2\text{ fit}} = 0.17 \tag{3.2}$$

and

$$\sigma(C_9)\big|_{z^2\text{ fit}} = 0.19 \qquad \text{and} \qquad \sigma(C_9)\big|_{z^3\text{ fit}} = 0.69\,. \tag{3.3}$$

Our findings can be summarised as follows:

- The impact of z^3 terms on the extraction of C_9 amounts to a shift by less than one standard deviation of the fit to order z^2, when considering data set sizes up to the LHCb Run-II size.
- The model-dependence due to the truncation of the series expansion at order z^2 is large in the absence of any theory constraints on the parameters $\{\alpha_k^{(\lambda)}\}$.

We conclude that a small model-dependence can only be achieved by using more information than only the experimental data of the semileptonic decay $B \to K^*\mu^+\mu^-$. However, when using order z^3 or higher, the current set of theoretical and experimental constraints does not allow for a staged approach [10], in which the posterior of a C_9-agnostic fit is used as a prior for the NP fit. We see three possibilities to overcome this problem:

JHEP10(2019)236

1. through a *staged* analysis that uses theoretical predictions beyond what has been discussed in [10] (e.g. lattice QCD calculations of the hadronic correlator on or in between the narrow charmonium resonances);

2. through a *simultaneous* analysis of the semimuonic *and* semielectronic decays, in which the parameters for the non-local matrix elements are shared (as shown in [36]);

3. through a *combined* analysis of the theory predictions at negative q^2, the measurements of the hadronic decays $B \to K^*\{J/\psi, \psi(2S)\}$, *and* the measurements of the semileptonic decays. This approach is investigated in the next section.

4 Combined unbinned analysis

In this section we extend our previous analysis by performing a combined unbinned fit of the theory predictions at negative q^2, the measurements of the hadronic decays $B \to K^*\{J/\psi, \psi(2S)\}$, and the measurements of the semileptonic decays. We investigate the following points:

A. Can the residual model-bias seen in section 3.3 be reduced by including theoretical predictions and measurements of the hadronic decays $B \to K^*\{J/\psi, \psi(2S)\}$?

B. What is the individual impact of the theoretical predictions and the hadronic decays inputs?

C. In this combined analysis, how does the residual model-bias depend on the values of the non-local hadronic parameters?

D. What are the prospects for a simultaneous fit to the WCs $\mathcal{C}_9^{\rm NP}$ and $\mathcal{C}_{10}^{\rm NP}$?

E. What is the gain in precision when determining the shape of the q^2-differential angular observables compared to binned analyses?

4.1 Combined fit to theory points at $q^2 < 0$, hadronic and semileptonic decays

In order to perform a combined fit to all the available (theoretical and experimental) information, we extend the current framework to include the predictions on the hadronic correlator calculated for points at negative q^2 and the two sets of pseudo-observables (three magnitudes and two relative phases for each of the J/ψ and $\psi(2S)$ resonances), as in [10]. Both contributions are included in the fit as multivariate Gaussians of the relevant pseudo-observables. For the production of the ensembles the corresponding central values are shifted to match their predictions given a certain set of parameters $\{\alpha_k^{(\lambda)}\}$, while the uncertainty is scaled to keep the relative error constant. Unless stated otherwise, ensembles are drawn from the BMP scenario, i.e. all the coefficients $\{\alpha_k^{(\lambda)}\}$ of order higher than z^2 are set to zero.

We explore the model-bias introduced by the truncation of the series by repeating the fit with different truncation orders for the z expansion. Two sets of toy analyses with 500

JHEP10(2019)236

	LHCb Run2 II		LHCb Upgrade [50 fb^{-1}]	
	Re $\mathcal{C}_9^{\rm NP}$ mean	Re $\mathcal{C}_9^{\rm NP}$ sigma	Re $\mathcal{C}_9^{\rm NP}$ mean	Re $\mathcal{C}_9^{\rm NP}$ sigma
z^2 fit	-0.966 ± 0.006	0.120 ± 0.004	-0.996 ± 0.003	0.060 ± 0.002
z^3 fit	-0.991 ± 0.011	0.217 ± 0.008	-1.015 ± 0.006	0.124 ± 0.004
z^4 fit	-1.022 ± 0.011	0.229 ± 0.008	-1.012 ± 0.007	0.146 ± 0.005
z^5 fit	-0.942 ± 0.016	0.293 ± 0.011	-0.983 ± 0.008	0.157 ± 0.006

Table 2. Expected central value and uncertainties for the $\mathcal{C}_9^{\rm NP}$ observable obtained from z^2, z^3, z^4 and z^5 fits for the BMP scenario with Re $\mathcal{C}_9^{\rm NP} = -1$.

ensembles each are produced, with data sets corresponding to the LHCb Run II and LHCb Upgrade [50 fb^{-1}] luminosity, respectively.

In table 2 we report the resulting sensitivity to the $\mathcal{C}_9^{\rm NP}$ obtained for z^2, z^3, z^4 and z^5 fits. Our findings can be summarised as follows:

- The uncertainty on $\mathcal{C}_9^{\rm NP}$ roughly doubles moving from z^2 fits to z^3 fits, for both statistics under consideration.
- For the dataset corresponding to the expected statistics at the LHCb Upgrade [50 fb^{-1}], the uncertainty on $\mathcal{C}_9^{\rm NP}$ slightly increases for orders higher than z^3.
- For the dataset corresponding to the expected statistics at the LHCb Run II we observe the saturation of the uncertainty at the orders z^3 and z^4. However, for the fit with z^5 the uncertainty starts to increase, pointing to a statistical limitation.

The observed distributions of the hadronic correlator $\mathcal{H}_\lambda(q^2)/\mathcal{F}_\lambda(q^2)$ for different orders in z are shown in figure 1, corresponding to the statistics expected at the LHCb Upgrade [50 fb^{-1}]. In all cases, the uncertainty drastically increases for higher orders in the $\psi(2S)$ window. For the regions Q_1 and Q_2, however, we find that the behaviour observed for $\mathcal{C}_9^{\rm NP}$ is reflected in the real part of the hadronic correlator, i.e. the uncertainty mildly increases for orders higher than z^3.

4.2 Exploring the impact of the inputs from theory and hadronic decays

We further investigate the impact of the additional pseudo-observables introduced in the combined fit, to distinguish the benefits obtained from either of the two inputs. In particular, we investigate the following questions:

- Is it possible to perform a purely experimental analysis, i.e., excluding the theoretical points at negative q^2 and relying only on semileptonic and hadronic decays?
- The pseudo-observables obtained for the hadronic decays currently constrain only two relative phase between the three polarisations. What is the impact of a hypothetical theory determination of the absolute phase of the hadronic decays or an increased precision of the relative phases?

JHEP10(2019)236

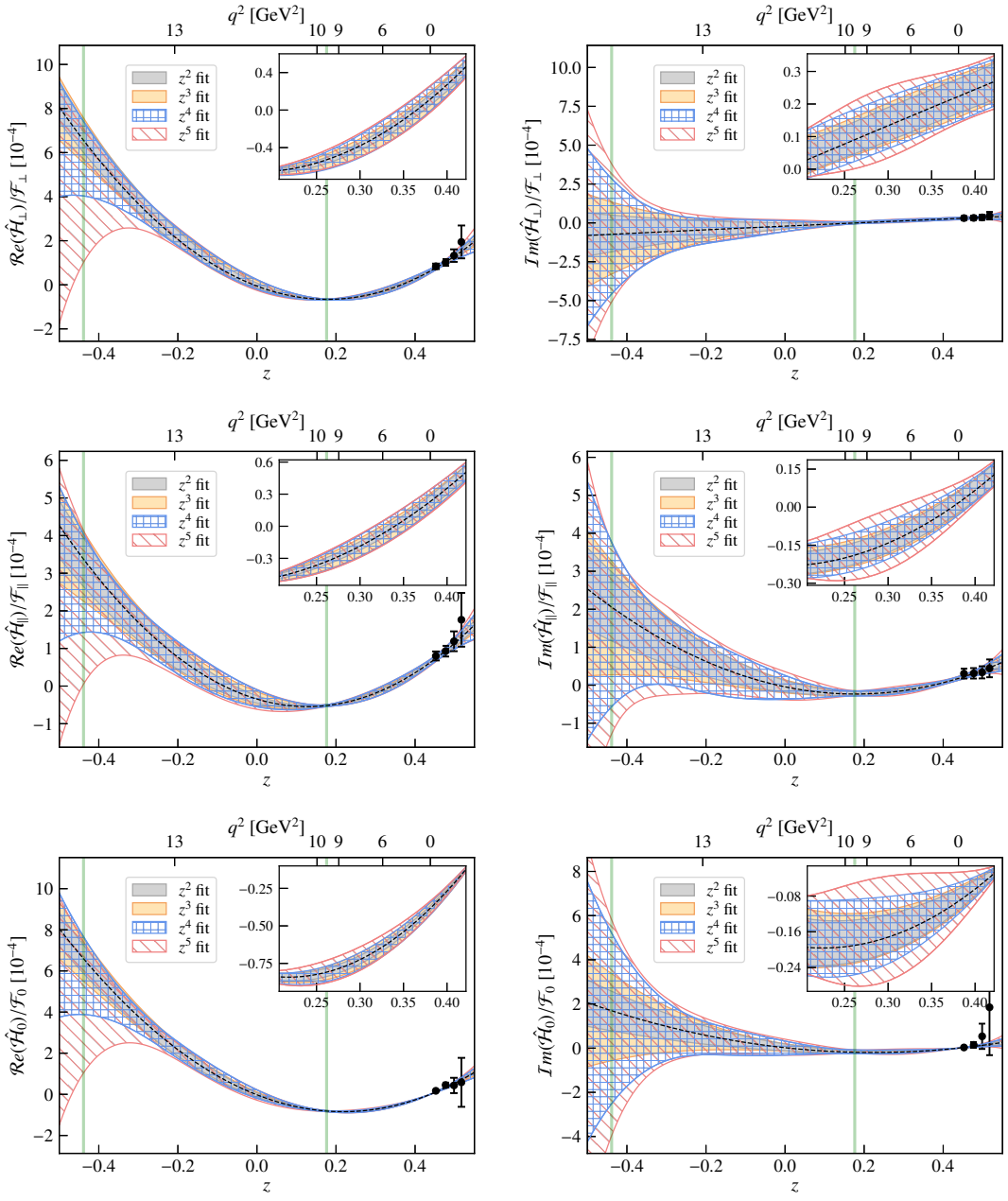

Figure 1. Results of the fits for the ratio Re $\hat{\mathcal{H}}_\lambda(z)/\mathcal{F}_\lambda(z)$ obtained with different orders of the expansion for the BMP scenario and the expected statistics at LHCb Upgrade [50 fb^{-1}]. The vertical bands correspond to the J/ψ and $\psi(2S)$ regions; the points to the theoretical inputs at negative q^2. The top right box of each plot zooms in the q^2 range between 1.1 and 9.0 GeV^2.

To address the first point we repeat the analysis removing the constraints introduced by the theoretical calculation at negative q^2, and we examine the stability of the fit scanning different orders of the expansion. We consider the BMP scenario corresponding to the expected statistics at LHCb Upgrade [50 fb^{-1}]. Figure 2 shows the result of the fit assuming z^4 truncation of the expansion performed with and without the input from the theory

JHEP10(2019)236

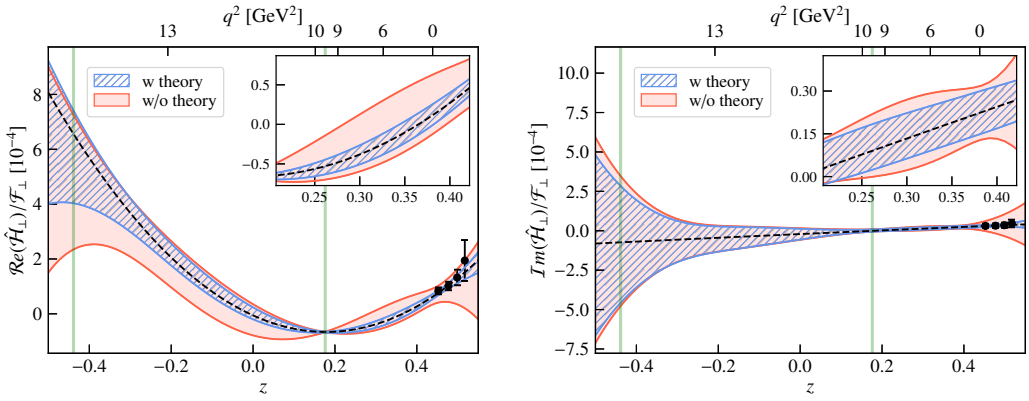

Figure 2. Results of the fits for the ratios $\hat{\mathcal{H}}_\perp(z)/\mathcal{F}_\perp(z)$ obtained with and without the theoretical points calculated at negative q^2. Fits correspond to the BMP scenario, the expected statistics at LHCb Upgrade [50 fb^{-1}] and to z^4 truncation in the series expansion. The vertical bands correspond to the J/ψ and $\psi(2S)$ regions; the points to the theoretical inputs at negative q^2. The top right box of each plot zooms in the q^2 range between 1.1 and 9.0 GeV^2.

points. We find a strong model-bias, similarly to what is presented in section 3.3. We conclude that a purely experimental analysis that combines information from the semileptonic decay and the hadronic $B \to K^*\{J/\psi, \psi(2S)\}$ decays is not currently possible. The desired disentangling of the hadronic effect from possible NP contributions crucially relies on the theory inputs from the points at negative q^2.

We investigate the benefits from hypothetical improvements to the constraints based on the hadronic decays. First of all we note that, as shown in figure 1, the uncertainty on the hadronic correlator evaluated at the J/ψ is extremely small. This is an intrinsic property of the analytical parametrisation, given by the change of one unit of π in the phase of the amplitude when crossing the resonance pole. We find that, for datasets corresponding to the expected statistics at LHCb Run II, the impact of the pseudo-observables of the J/ψ improves the determination of the WC C_9 by approximately 15%, while it plays a minor role when increasing the z-expansion to higher orders. Furthermore, the fit is able to select the absolute phase of the J/ψ with the same precision as the two relative phases. Secondly, the impact of the $\psi(2S)$ pseudo-observables on the combined fit is of great interest since these are weakly constrained, in particular the two relative phases [10]. We test whether it would be beneficial to have a measurement of the absolute phase of the $\psi(2S)$ and/or assuming future improvement in the determination of the pseudo-observables of the $\psi(2S)$. We proceed inserting a hypothetical constraint on the absolute phase of the $\psi(2S)$ and repeating the analysis with two configurations: first, we assume the relative uncertainty of the absolute phase of the $\psi(2S)$ of the same order as the one of relative phases. Second, we reduce the uncertainties of all phases of the $\psi(2S)$ to reflect the uncertainties of the J/ψ. In both cases the central value of the absolute phase of the $\psi(2S)$ is set to the prediction obtained from the default set of parameters $\{\alpha_k^{(\lambda)}\}$ used for the production of the ensembles.

JHEP10(2019)236

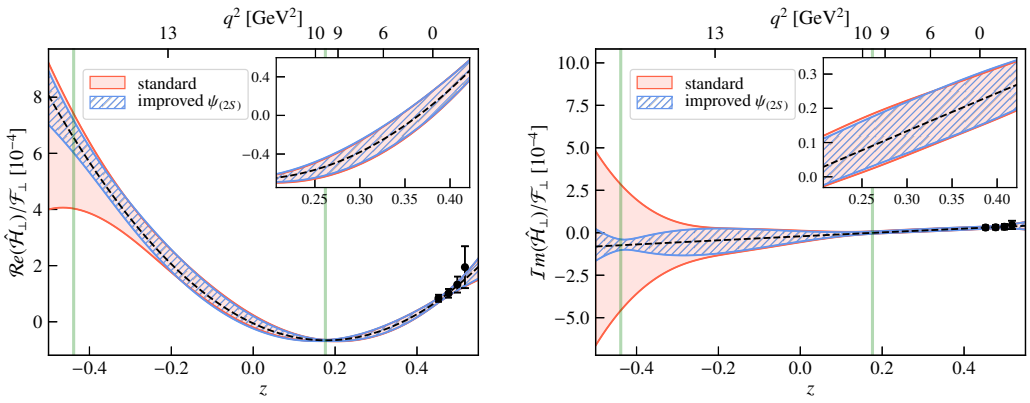

Figure 3. Results of the fits for the ratios $\hat{\mathcal{H}}_\perp(z)/\mathcal{F}_\perp(z)$ obtained with the current status of the theoretical and experimental knowledge and assuming future improvements on the $B \to K^*\psi(2S)$ measurements. Fits correspond to the BMP scenario, the expected statistics at LHCb Upgrade [50 fb^{-1}] and to z^4 truncation in the series expansion. The vertical bands correspond to the J/ψ and $\psi(2S)$ regions; the points to the theoretical inputs at negative q^2. The top right box of each plot zooms in the q^2 range between 1.1 and 9.0 GeV^2.

We find that, even assuming the best case, the improvements on the determination of the WC $\mathcal{C}_9^{\rm NP}$ are negligible. Figure 3 shows the comparison of the results obtained for the hadronic correlator for the analysis carried out with all the currently available information and the analysis that assumes the future improvements on the $\psi(2S)$ described above. Both analyses are performed with datasets corresponding to the LHCb Upgrade [50 fb^{-1}] expected statistics and assume the z^4 truncation in the series expansion. We find that the benefits produced by the assumed improvements on the $\psi(2S)$ pseudo-observables are limited to the region of the $\psi(2S)$.

4.3 On the truncation of the series at z^K

All the studies presented so far assumed a fixed set of initial values for the parameters $\{\alpha_k^{(\lambda)}\}$ in the production of the ensembles (obtained from [10]), in this section we investigate the effect on the fit results of a different choice for the initial values of the hadronic parameters. We investigate two options. First, we produce ensembles with non-zero coefficients for order of the expansion up to z^3 (i.e. $\alpha_{i\geq 4}^{(\lambda)} = 0$). Second, we produce ensembles with non-zero coefficients for order of the expansion up to z^4 (i.e. $\alpha_{i\geq 5}^{(\lambda)} = 0$).

The choice of the above-mentioned non-zero coefficients is based on the following criteria: they must be realistic (i.e. compatible the theory predictions at negative q^2 and the pseudo-observables from the hadronic decays) and reduce the tension with the P_5' anomaly (i.e. hadronic effects mimic the behaviour of NP). The resulting set of parameters is shown in figure 4 together with the value of the P_5' angular observable obtained in the different cases.

For each of the two generated configurations we perform the analysis as described in section 4.1, repeating the fit by varying the truncation of the expansion from z^2 to z^5. Results are shown in tables 3 and 4, respectively.

JHEP10(2019)236

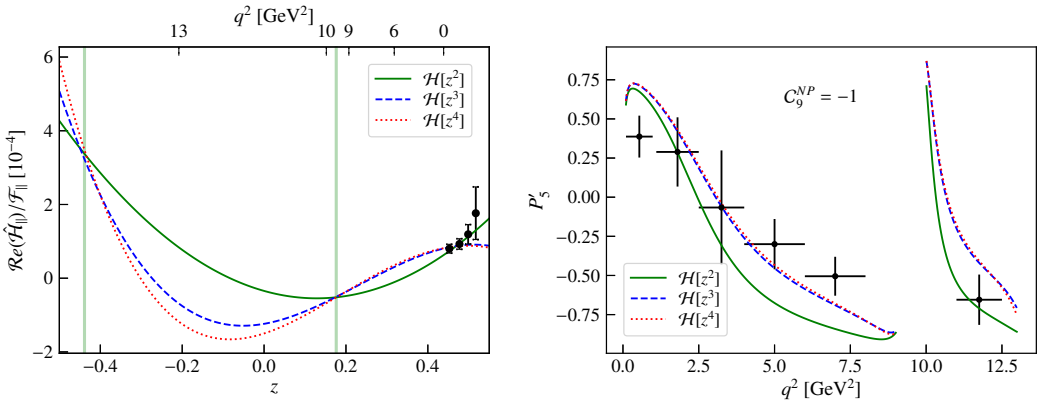

Figure 4. Left: $\mathrm{Re}\hat{\mathcal{H}}_\parallel(z)/\mathcal{F}_\parallel(z)$ corresponding to the set of parameter $\{\alpha_k^{(\parallel)}\}$ used for the production of the ensembles in the different hypotheses as described in the text. Right: projection of the different hypotheses in the P_5' angular observable, all the three configurations assumes the BMP scenario. The result of the LHCb Run I analysis [2] is overlaid as reference.

	LHCb Run II		LHCb Upgrade [50 fb^{-1}]	
	$\mathrm{Re}\,\mathcal{C}_9^{\mathrm{NP}}$ mean	$\mathrm{Re}\,\mathcal{C}_9^{\mathrm{NP}}$ sigma	$\mathrm{Re}\,\mathcal{C}_9^{\mathrm{NP}}$ mean	$\mathrm{Re}\,\mathcal{C}_9^{\mathrm{NP}}$ sigma
z^2 fit	-1.709 ± 0.007	0.138 ± 0.005	-1.721 ± 0.003	0.060 ± 0.002
z^3 fit	-1.004 ± 0.010	0.200 ± 0.007	-1.021 ± 0.005	0.106 ± 0.004
z^4 fit	-1.046 ± 0.011	0.214 ± 0.008	-1.013 ± 0.006	0.123 ± 0.004
z^5 fit	-0.946 ± 0.013	0.258 ± 0.009	-0.986 ± 0.007	0.144 ± 0.005

Table 3. Expected central value and uncertainties for the $\mathcal{C}_9^{\mathrm{NP}}$ observable obtained from z^2, z^3, z^4 and z^5 fits for the BMP scenario when produced with non-zero z^3 coefficients as described in the text.

Our conclusion can be summarised as follows:

- fitting with the expansion truncated at z^2 (i.e. lower order than what is used for the production of the ensembles) introduces a strong bias in the estimator for $\mathcal{C}_9^{\mathrm{NP}}$;
- when the order of the truncation in the fitting procedure catches up the one used for the production of the ensembles the estimator for $\mathcal{C}_9^{\mathrm{NP}}$ is unbiased;
- the uncertainty on $\mathcal{C}_9^{\mathrm{NP}}$ varying the order of the fit follows the pattern observed in section 4.1.
- our lack of knowledge on the real description of the hadronic effects in nature can be investigated by scanning the order of the truncation of the series until the central value of $\mathcal{C}_9^{\mathrm{NP}}$ stabilises. Obviously, this procedure is bounded to the limit of the available statistics.

4.4 Simultaneous fit to $\mathcal{C}_9^{\mathrm{NP}}$ and $\mathcal{C}_{10}^{\mathrm{NP}}$

As mentioned in section 2, $\mathcal{C}_{10}^{\mathrm{NP}}$ does not suffer from pollution from hadronic non-local effects. Nevertheless, it is interesting to extend the explored WCs parameter space and

JHEP10(2019)236

	LHCb Run II		LHCb Upgrade [50 fb^{-1}]	
	Re $\mathcal{C}_9^{\rm NP}$ mean	Re $\mathcal{C}_9^{\rm NP}$ sigma	Re $\mathcal{C}_9^{\rm NP}$ mean	Re $\mathcal{C}_9^{\rm NP}$ sigma
z^2 fit	-1.813 ± 0.007	0.136 ± 0.005	-1.824 ± 0.003	0.063 ± 0.002
z^3 fit	-1.094 ± 0.010	0.196 ± 0.007	-1.188 ± 0.005	0.103 ± 0.004
z^4 fit	-1.049 ± 0.010	0.205 ± 0.007	-1.018 ± 0.006	0.119 ± 0.004
z^5 fit	-0.938 ± 0.013	0.257 ± 0.009	-0.985 ± 0.007	0.141 ± 0.005

Table 4. Expected central value and uncertainties for the $\mathcal{C}_9^{\rm NP}$ observable obtained from z^2, z^3, z^4 and z^5 fits for the BMP scenario when produced with non-zero z^4 coefficients as described in the text.

	LHCb Run II				
	Re $\mathcal{C}_9^{\rm NP}$ mean	Re $\mathcal{C}_9^{\rm NP}$ sigma	Re $\mathcal{C}_{10}^{\rm NP}$ mean	Re $\mathcal{C}_{10}^{\rm NP}$ sigma	correlation Re $\mathcal{C}_9^{\rm NP}$–Re $\mathcal{C}_{10}^{\rm NP}$
z^2 fit	-0.982 ± 0.008	0.164 ± 0.006	0.032 ± 0.010	0.204 ± 0.007	-0.680
z^3 fit	-1.029 ± 0.012	0.244 ± 0.009	0.060 ± 0.010	0.207 ± 0.007	-0.465
z^4 fit	-1.053 ± 0.013	0.253 ± 0.009	0.051 ± 0.011	0.223 ± 0.008	-0.427
z^5 fit	-0.983 ± 0.017	0.312 ± 0.012	0.091 ± 0.013	0.254 ± 0.009	-0.400

Table 5. Fit results obtained when floating $\mathcal{C}_9^{\rm NP}$ and $\mathcal{C}_{10}^{\rm NP}$ for z^2, z^3, z^4 and z^5 fits. Ensembles are produced for the BMP scenario with the corresponding statistics expected at the LHCb Run II.

study the effect of floating $\mathcal{C}_9^{\rm NP}$ and $\mathcal{C}_{10}^{\rm NP}$ simultaneously in the fit. We repeat the analysis as in section 4.1, producing 500 ensembles assuming the BMP scenario (with NP inserted only in $\mathcal{C}_9^{\rm NP}$, i.e. $\mathcal{C}_{10}^{\rm NP} = 0$) with z^2 and performing the fit with truncation at the order z^2, z^3, z^4 and z^5. The 2D pulls are shown in figure 5 while the single projections are reported in tables 5 and 6. Figure 6 shows the same result for different datasets corresponding to the expected statistics at LHCb Run II, LHCb Upgrade [50 fb^{-1}–300 fb^{-1}] and Belle II [50 ab^{-1}]. For simplicity, only the results obtained from the z^3 analysis are shown.

We note that:

- The uncertainty on $\mathcal{C}_9^{\rm NP}$ varying the order of the fit follows the pattern observed in section 4.1;

- due to the correlation between $\mathcal{C}_9^{\rm NP}$ and $\mathcal{C}_{10}^{\rm NP}$ the projection of the uncertainty on the single WC $\mathcal{C}_9^{\rm NP}$ is larger compared to the case of section 4.1 when $\mathcal{C}_{10}^{\rm NP}$ was fixed in the fit;

- besides the non-local hadronic effects, a precise determination of the WCs is limited by the uncertainties on the form factors, in particular, the precision on $\mathcal{C}_{10}^{\rm NP}$ already saturates with the statistics expected to be collected at LHCb Run II (see figure 6). The precision on $\mathcal{C}_{10}^{\rm NP}$ can be substantially improved by including constraints from the decay $B_s \to \mu^+\mu^-$.

JHEP10(2019)236

	LHCb Upgrade [50 fb^{-1}]				
	Re $\mathcal{C}_9^{\rm NP}$ mean	Re $\mathcal{C}_9^{\rm NP}$ sigma	Re $\mathcal{C}_{10}^{\rm NP}$ mean	Re $\mathcal{C}_{10}^{\rm NP}$ sigma	correlation Re $\mathcal{C}_9^{\rm NP}$- Re $\mathcal{C}_{10}^{\rm NP}$
z^2 fit	-1.005 ± 0.007	0.132 ± 0.005	0.014 ± 0.008	0.171 ± 0.006	-0.891
z^3 fit	-1.057 ± 0.010	0.193 ± 0.007	0.044 ± 0.009	0.188 ± 0.007	-0.791
z^4 fit	-1.041 ± 0.011	0.220 ± 0.008	0.037 ± 0.010	0.202 ± 0.007	-0.781
z^5 fit	-1.021 ± 0.011	0.228 ± 0.008	0.051 ± 0.010	0.207 ± 0.007	-0.734

Table 6. Fit results obtained when floating $\mathcal{C}_9^{\rm NP}$ and $\mathcal{C}_{10}^{\rm NP}$ for z^2, z^3, z^4 and z^5 fits. Ensembles are produced for the BMP scenario with the corresponding statistics expected at the LHCb Upgrade [50 fb^{-1}].

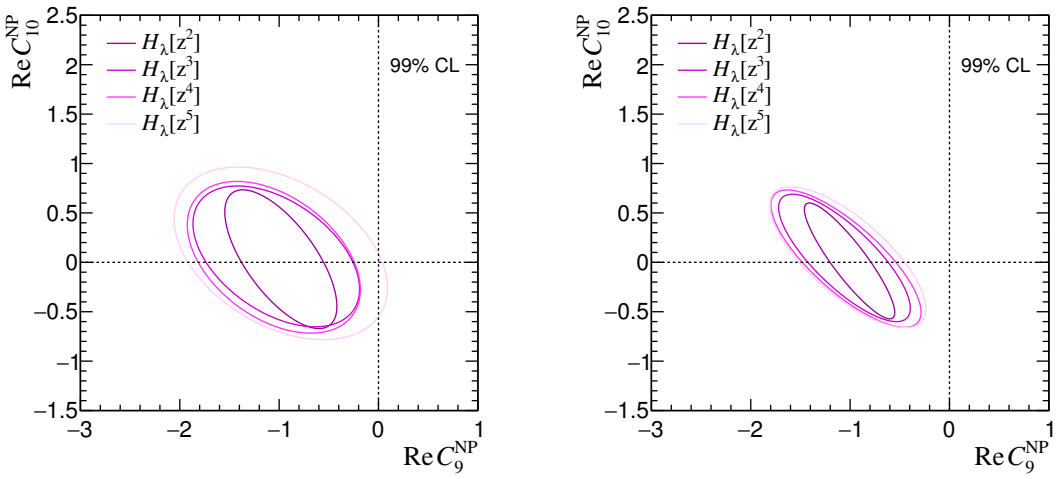

Figure 5. Two-dimensional sensitivity scans for the pair of Wilson coefficients $\mathcal{C}_9^{\rm NP}$ and $\mathcal{C}_{10}^{\rm NP}$ for different non-local hadronic parametrisation models. The contours correspond to $3\,\sigma$ statistical-only uncertainty bands evaluated with the expected statistics after LHCb Run II (left) and LHCb Upgrade [50 fb^{-1}] (right).

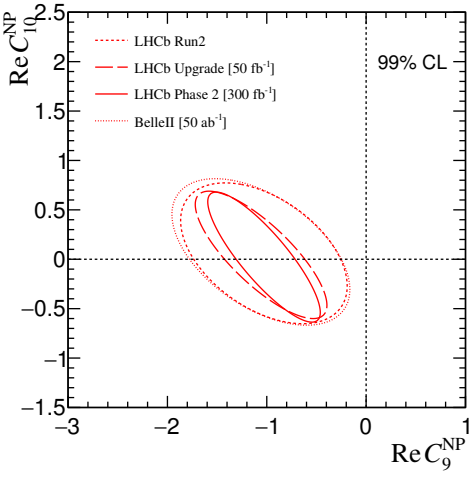

Figure 6. Two-dimensional sensitivity scans for the pair of Wilson coefficients $\mathcal{C}_9^{\rm NP}$ and $\mathcal{C}_{10}^{\rm NP}$ for the expected statistics corresponding to LHCb Run II (dotted), LHCb Upgrade [50 fb^{-1}] (dashed), LHCb Upgrade [300 fb^{-1}] (solid) and Belle II [50 ab^{-1}] (long dashed). The contours correspond to $3\,\sigma$ statistical-only uncertainty bands obtained with z^3 fits.

JHEP10(2019)236

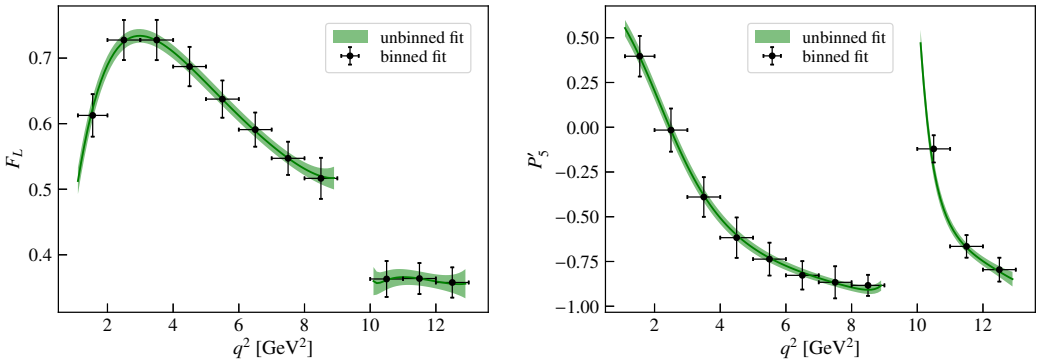

Figure 7. Angular observables F_L and P'^5 obtained a-posteriori from the unbinned amplitude fit results compared with the binned angular analysis. Both approaches analyse the same set of ensembles generated with the BMP scenario and the expected statistics at LHCb Run II.

4.5 Unbinned determination of angular observables

One of the benefits of our proposed approach is that it takes advantage of the full unbinned description of the decay and, additionally, the amplitude fit allows to reproduce confidence intervals for the commonly used angular observables. In the following we investigate the statistical uncertainty expected for the obtained angular observables. We perform the analysis on 500 ensembles generated with the expected statistics at LHCb Run II and we repeat the fit with different truncations at the z^2, z^3, z^4 and z^5 order. We find that the uncertainty on all the angular observables is independent on the assumption on the truncation of the series expansion, leading to clean results free from systematic uncertainties on the hadronic parametrisation. It is interesting to compare the statistical uncertainty on the angular observables obtained by the unbinned amplitude fit with respect to the binned approach. We perform a binned fit on the same ensembles generated above, splitting the datasets in $1\,\text{GeV}^2$ q^2 bins, and we fit the obtained angular distributions with the signal PDF $\text{d}^3\Gamma/\text{d}^3\Omega$ as described in [4]. Figure 7 shows the improvement on the statistical uncertainty on the angular observables obtained by the unbinned amplitude fit compared to a q^2 binned angular analysis.

5 Conclusion

Measurements of angular observables in the decay $B \to K^*\mu^+\mu^-$ have shown discrepancies with respect to Standard Model predictions, mainly in the angular observable known as P'_5. This anomaly has been widely discussed in the literature, in particular since non-local charm contributions are challenging to be predicted from a theory point of view. Here we carried out a sensitivity study of the decay $B \to K^*\mu^+\mu^-$, taking care to account for hadronic matrix elements of both local and non-local operators in a quasi-model-independent way. This is done by performing an extended unbinned maximum likelihood fit, which allows to use the full information of the data and extract simultaneously the hadronic parameters and the Wilson Coefficients. Other studies have proposed methods

JHEP10(2019)236

to disentangle NP from non-local hadronic effects in (un)binned likelihood fits. Following the parametrisation of ref. [10] we studied the properties of the fit for a large number of different scenarios, by using simulated pseudoexperiments. Fitting with the order of the z-expansion used in the production of the ensembles leads to an unbiased value of $\mathcal{C}_9^{\rm NP}$. Increasing the order of the z-expansion, the central value of $\mathcal{C}_9^{\rm NP}$ stays unbiased while the uncertainty increases. It is observed that theory constraints strongly mitigate this problem, limiting the deterioration of the uncertainty on $\mathcal{C}_9^{\rm NP}$ to $\mathcal{O}(10\%)$ for each order to the z-expansion added to the fit. The fact that the uncertainty on $\mathcal{C}_9^{\rm NP}$ steadily increases with the order of the polynomial of the z-expansion does not allow us to rigorously assign a systematic uncertainty due to the truncation of the z-expansion a-priori. We also found that the unbinned fit allows to extract additional information on the non-local matrix elements from semi-muonic decay events alone. Our study goes beyond previous works, and assesses in a quantitative way the model-dependency due to our ansatz for the non-local hadronic contributions. Our approach allows systematic improvements (through increasing the truncation order in z) and estimation of systematic uncertainties (through varying the truncation order even when the data is described well). In addition, the unbinned fit can be used for the determination of the usual angular observables with precision beyond what can be expected with the standard binned approach. We find that the angular observables obtained with this method do not exhibit any sizeable model bias due to the truncation of the z-expansion. It should be emphasised that the gain in sensitivity cannot be directly read from figure 7 since the points of the binned likelihood fit are all uncorrelated. To fully access the comparison of the two approaches, a binned fit to the angular observables with the same model should be performed.

While not strictly necessary, improving our knowledge of the $B \to K^*\psi(2S)$ amplitudes can give us greater confidence of the obtained fit results. We therefore encourage revisiting their analysis at the present B-physics experiments. The application of the unbinned fit for the decays $B \to K\mu^+\mu^-$ and $\Lambda_b \to \Lambda\mu^+\mu^-$ has not been studied here. It is unclear how the lack of phase information on the J/ψ and $\psi(2S)$ poles will affect the efficiency of the unbinned fit. We therefore encourage dedicated sensitivity studies for these decays as a natural extension of our present work.

Acknowledgments

We are grateful to Christoph Bobeth, Sébastien Descotes-Genon, Patrick Owen, and Javier Virto for useful discussions. We also thank Christoph Bobeth and Javier Virto for valuable comments on the manuscript. D.v.D. gratefully acknowledges partial support by the Swiss National Science Foundation (SNF) under contract 200021-159720, and by the Emmy Noether programme of the Deutsche Forschungsgemeinschaft (DFG) under grant DY 130/1-1. A.M., N.S. and R.S.C. also acknowledge the support by SNF under contracts 173104 and 174182. The work of M.C. is funded by the Polish National Agency for Academic Exchange under the Bekker program. M.C. is also grateful to Foundation for Polish Science (FNP) for its support.

JHEP10(2019)236

A Parametrisation of the non-local hadronic correlators $\mathcal{H}_\lambda(q^2)$

For completeness, the parametrisation of the non-local hadronic correlators $\mathcal{H}_\lambda(q^2)$ introduced in reference [10] is summarised in the following. The functions $\mathcal{H}_\lambda(q^2)$ are expressed in terms of the variable z, which is obtained via a conformal map of q^2,

$$z(q^2) \equiv \frac{\sqrt{t_+ - q^2} - \sqrt{t_+ - t_0}}{\sqrt{t_+ - q^2} + \sqrt{t_+ - t_0}}\,, \tag{A.1}$$

where $t_+ = 4M_D^2$ and $t_0 = t_+ - \sqrt{t_+(t_+ - M^2_{\psi(2S)})}$. This transformation leads to the functions $\mathcal{H}_\lambda(z)$, which are meromorphic in $|z| < 1$ and have two simple poles at $z_{J/\psi} \simeq 0.18$ and $z_{\psi(2S)} \simeq -0.44$. Therefore, dividing out these singularities gives analytic functions in $|z| < 1$ that can be Taylor-expanded around $z = 0$. In summary, the non-local correlators are parametrised as

$$\mathcal{H}_\lambda(z) = \frac{1 - z z^*_{J/\psi}}{z - z_{J/\psi}} \frac{1 - z z^*_{\psi(2S)}}{z - z_{\psi(2S)}} \hat{\mathcal{H}}_\lambda(z) \qquad \text{with} \qquad \hat{\mathcal{H}}_\lambda(\mathrm{z}) = \left[\sum_{\mathrm{k}=0}^{\mathrm{K}} \alpha_{\mathrm{k}}^{(\lambda)} \mathrm{z}^{\mathrm{k}}\right] \mathcal{F}_\lambda(\mathrm{z})\,. \tag{A.2}$$

B S-wave contribution

The contribution of events with the $K\pi$ system in a scalar (S-wave) configuration has been measured to be small, below 10% in the range $796 < m_{K\pi} < 996\,\mathrm{MeV}$ [37]. Nevertheless, it can dilute the sensitivity to $B^0 \to K^{*0}\mu^+\mu^-$ decays and pollute the observables of interest [38, 39]. To appropriately take this contribution into account, additional complex amplitudes $A_S^{L,R}$ must be included in the decay rate. These follow ref. [40] and are modified accordingly to eq. (2.2) to coherently include non-local hadronic effects in the S-wave as well, resulting in

$$\begin{aligned}
\mathcal{A}_{S0}^{L,R} &= -\mathcal{N}_0 \frac{\sqrt{\lambda_{K_0^*}}}{M_B\sqrt{q^2}} \left\{ (\mathcal{C}_9 \mp \mathcal{C}_{10}) f_+(q^2) + \frac{2m_b M_B}{q^2} \left[\mathcal{C}_7 f_T(q^2) - 16\pi^2 \frac{M_B}{m_b} \mathcal{H}_S(q^2) \right] \right\}, \\
\mathcal{A}_{St} &= -2\mathcal{N}_0 \frac{M_B^2 - M_{K_0^*}^2}{M_B\sqrt{q^2}} \mathcal{C}_{10} f_0(q^2),
\end{aligned} \tag{B.1}$$

Three new form factors are required to parametrise the scalar $B \to K_0^*$ transition matrix elements, namely f_+, f_T and f_0, whose definitions slightly differ from ref. [40] and are determined by the following matrix elements,

$$\langle K_0^*(k)|\bar{s}\gamma_\mu\gamma_5 b|B(p)\rangle = \left[(p+k)_\mu - \frac{M_B^2 - M_{K_0^*}^2}{q^2} q_\mu\right] f_+(q^2) + \frac{M_B^2 - M_{K_0^*}^2}{q^2} q_\mu\, f_0(q^2) \tag{B.2}$$

and

$$\langle K_0^*(k)|\bar{s}\sigma_{\mu\nu}\gamma_5 q^\nu b|B(p)\rangle = i\Big[(M_B^2 - M_{K_0^*}^2) q_\mu - q^2 (p+k)_\mu\Big] \frac{M_B}{q^2} f_T(q^2)\,. \tag{B.3}$$

The non-local hadronic functions $\mathcal{H}_S(q^2)$ follow eq. (A.2) with the replacement

$$\hat{\mathcal{H}}_S(z) = \left[\sum_{k=0}^{K} \alpha_k^S z^k\right] f_+(q^2)\,. \tag{B.4}$$

JHEP10(2019)236

In summary, the described parametrisation introduces a new set of complex parameters $\{\alpha_k^{S0}\}$ to characterise the non-local hadronic contributions to the S-wave and guarantees a uniform formalism between P- and S-wave decays.

In order to inspect the S-wave contribution in the considered $K^+\pi^-$ mass region, the invariant mass of the $K^+\pi^-$ system is included in the fit. The different amplitudes are then modified as follows

$$\begin{aligned} A_\lambda^{L,R}(q^2, m_{K\pi}^2) &= A_\lambda^{L,R}(q^2) \times f_{892}(m_{K\pi}^2)\,, \\ A_{S\lambda}^{L,R}(q^2, m_{K\pi}^2) &= A_{S\lambda}^{L,R}(q^2) \times f_{K_0^*}(m_{K\pi}^2)\,, \end{aligned} \tag{B.5}$$

with

$$\begin{aligned} f_{892}(m_{K\pi}^2) &= \mathcal{N}_{\rm BW} \cdot f_{\rm BW}(m_{K\pi}^2)\,, \\ f_{K_0^*}(m_{K\pi}^2) &= \mathcal{N}_{\rm LASS} \cdot |g_S| e^{i\delta_S} \cdot f_{\rm LASS}(m_{K\pi}^2)\,, \end{aligned} \tag{B.6}$$

where $f_{\rm BW}(m_{K\pi}^2)$ is a relativistic Breit-Wigner, $f_{\rm LASS}(m_{K\pi}^2)$ is the LASS lineshape [41], $\mathcal{N}_{\rm BW}$ and $\mathcal{N}_{\rm LASS}$ are normalisation factors and the coefficients g_S and δ_S determine the relative magnitude and phase between P and S-contributions.

The generation of ensembles follows the guidelines of section 2 with the following additional conditions:

- the S-wave relative magnitude is set to $g_S = 0.93$, which corresponds to an averaged S-wave fraction compatible with ref. [37], while the relative phase is arbitrarily set to $\delta_S = \pi/2$;
- the scalar form factors f_+, f_T and f_0 are parametrised as in [42];
- the values of the S-wave non-local hadronic parameters $\{\alpha_k^S\}$ are set identically to the ones of the longitudinal P-wave polarisation, $\{\alpha_k^0\}$, furthermore, the truncation of the S-wave non-local hadronic functions $\mathcal{H}_S$ is aligned to the same order considered for the corresponding P-wave functions.

All the above S-wave parameters are let floating freely in the fit except for the S-wave form factors, which are Gaussian constrained based on the results of ref. [42] with the uncertainties enlarged by a factor of 3 in order to take into account differences between $B^0 \to K_0^*$ and $B^+ \to K^+$ dynamics. We find that this conservative choice has a negligible impact on the determination of the parameters of interest, due to the limited amount of S-wave contribution.

Table 7 reports the fit results for the WCs $\mathcal{C}_9$ and $\mathcal{C}_{10}$ obtained with fits with z^2 to 500 ensembles produced with the expected statistics at LHCb Run II and the BMP scenario. We note that, despite the large number of additional parameters, the precision on the determination of the WCs remains approximately unchanged when including the S-wave contribution. This result further increases the confidence that a direct determination the Wilson coefficients $\mathcal{C}_9$ and $\mathcal{C}_{10}$ through an amplitude fit to $B \to K^*\mu^+\mu^-$ decays is possible.

JHEP10(2019)236

	LHCb Run II				
	$\mathrm{Re}\,\mathcal{C}_9^{\mathrm{NP}}$ mean	$\mathrm{Re}\,\mathcal{C}_9^{\mathrm{NP}}$ sigma	$\mathrm{Re}\,\mathcal{C}_{10}^{\mathrm{NP}}$ mean	$\mathrm{Re}\,\mathcal{C}_{10}^{\mathrm{NP}}$ sigma	correlation $\mathrm{Re}\,\mathcal{C}_9^{\mathrm{NP}}$–$\mathrm{Re}\,\mathcal{C}_{10}^{\mathrm{NP}}$
P-wave	-0.982 ± 0.008	0.164 ± 0.006	0.032 ± 0.010	0.204 ± 0.007	-0.680
S+P-waves	-0.976 ± 0.008	0.169 ± 0.005	0.029 ± 0.010	0.224 ± 0.007	-0.67

Table 7. Fit results obtained when floating $\mathcal{C}_9^{\mathrm{NP}}$ and $\mathcal{C}_{10}^{\mathrm{NP}}$ for z^2 fits. Ensembles are produced for the BMP scenario with the corresponding statistics expected at the LHCb Run II.

References

[1] LHCb collaboration, *Implications of LHCb measurements and future prospects*, *Eur. Phys. J.* **C 73** (2013) 2373 [arXiv:1208.3355] [INSPIRE].

[2] LHCb collaboration, *Measurement of form-factor-independent observables in the decay* $B^0 \to K^{*0}\mu^+\mu^-$, *Phys. Rev. Lett.* **111** (2013) 191801 [arXiv:1308.1707] [INSPIRE].

[3] S. Descotes-Genon, J. Matias, M. Ramon and J. Virto, *Implications from clean observables for the binned analysis of* $B \to K*\mu^+\mu^-$ *at large recoil*, *JHEP* **01** (2013) 048 [arXiv:1207.2753] [INSPIRE].

[4] LHCb collaboration, *Angular analysis of the* $B^0 \to K^{*0}\mu^+\mu^-$ *decay using 3* fb^{-1} *of integrated luminosity*, *JHEP* **02** (2016) 104 [arXiv:1512.04442] [INSPIRE].

[5] BELLE collaboration, *Lepton-flavor-dependent angular analysis of* $B \to K^*\ell^+\ell^-$, *Phys. Rev. Lett.* **118** (2017) 111801 [arXiv:1612.05014] [INSPIRE].

[6] G. Hiller and F. Krüger, *More model-independent analysis of* $b \to s$ *processes*, *Phys. Rev.* **D 69** (2004) 074020 [hep-ph/0310219] [INSPIRE].

[7] LHCb collaboration, *Test of lepton universality using* $B^+ \to K^+\ell^+\ell^-$ *decays*, *Phys. Rev. Lett.* **113** (2014) 151601 [arXiv:1406.6482] [INSPIRE].

[8] LHCb collaboration, *Test of lepton universality with* $B^0 \to K^{*0}\ell^+\ell^-$ *decays*, *JHEP* **08** (2017) 055 [arXiv:1705.05802] [INSPIRE].

[9] C. Bobeth, G. Hiller and D. van Dyk, *General analysis of* $\bar{B} \to \bar{K}^{(*)}\ell^+\ell^-$ *decays at low recoil*, *Phys. Rev.* **D 87** (2013) 034016 [arXiv:1212.2321] [INSPIRE].

[10] C. Bobeth, M. Chrzaszcz, D. van Dyk and J. Virto, *Long-distance effects in* $B \to K^*\ell\ell$ *from analyticity*, *Eur. Phys. J.* **C 78** (2018) 451 [arXiv:1707.07305] [INSPIRE].

[11] A. Ali, G.F. Giudice and T. Mannel, *Towards a model independent analysis of rare B decays*, *Z. Phys.* **C 67** (1995) 417 [hep-ph/9408213] [INSPIRE].

[12] G. Buchalla, A.J. Buras and M.E. Lautenbacher, *Weak decays beyond leading logarithms*, *Rev. Mod. Phys.* **68** (1996) 1125 [hep-ph/9512380] [INSPIRE].

[13] M. Beneke, T. Feldmann and D. Seidel, *Systematic approach to exclusive* $B \to Vl^+l^-$, $V\gamma$ *decays*, *Nucl. Phys.* **B 612** (2001) 25 [hep-ph/0106067] [INSPIRE].

[14] M. Beneke, T. Feldmann and D. Seidel, *Exclusive radiative and electroweak* $b \to d$ *and* $b \to s$ *penguin decays at NLO*, *Eur. Phys. J.* **C 41** (2005) 173 [hep-ph/0412400] [INSPIRE].

[15] A. Khodjamirian, T. Mannel, A.A. Pivovarov and Y.M. Wang, *Charm-loop effect in* $B \to K^{(*)}\ell^+\ell^-$ *and* $B \to K^*\gamma$, *JHEP* **09** (2010) 089 [arXiv:1006.4945] [INSPIRE].

JHEP10(2019)236

[16] J. Lyon and R. Zwicky, *Resonances gone topsy turvy - the charm of QCD or new physics in $b \to s\ell^+\ell^-$?*, arXiv:1406.0566 [INSPIRE].

[17] M. Ciuchini et al., *$B \to K^*\ell^+\ell^-$ decays at large recoil in the standard model: a theoretical reappraisal*, *JHEP* **06** (2016) 116 [arXiv:1512.07157] [INSPIRE].

[18] LHCb collaboration, *Measurement of the phase difference between short- and long-distance amplitudes in the $B^+ \to K^+\mu^+\mu^-$ decay*, *Eur. Phys. J.* **C 77** (2017) 161 [arXiv:1612.06764] [INSPIRE].

[19] M. Ciuchini et al., *On flavourful easter eggs for new physics hunger and lepton flavour universality violation*, *Eur. Phys. J.* **C 77** (2017) 688 [arXiv:1704.05447] [INSPIRE].

[20] T. Blake, U. Egede, P. Owen, K.A. Petridis and G. Pomery, *An empirical model to determine the hadronic resonance contributions to $\overline{B}^0 \to \overline{K}^{*0}\mu^+\mu^-$ transitions*, *Eur. Phys. J.* **C 78** (2018) 453 [arXiv:1709.03921] [INSPIRE].

[21] F. Krüger, L.M. Sehgal, N. Sinha and R. Sinha, *Angular distribution and CP asymmetries in the decays $\bar{B} \to K^-\pi^+e^-e^+$ and $\bar{B} \to \pi^-\pi^+e^-e^+$*, *Phys. Rev.* **D 61** (2000) 114028 [*Erratum ibid.* **D 63** (2001) 019901] [hep-ph/9907386] [INSPIRE].

[22] F. Krüger and J. Matias, *Probing new physics via the transverse amplitudes of $B^0 \to K^{*0}(\to K^-\pi^+)l^+l^-$ at large recoil*, *Phys. Rev.* **D 71** (2005) 094009 [hep-ph/0502060] [INSPIRE].

[23] M. Dimou, J. Lyon and R. Zwicky, *Exclusive chromomagnetism in heavy-to-light FCNCs*, *Phys. Rev.* **D 87** (2013) 074008 [arXiv:1212.2242] [INSPIRE].

[24] C. Bobeth, G. Hiller and G. Piranishvili, *CP asymmetries in bar $B \to \bar{K}^*(\to \bar{K}\pi)\bar{\ell}\ell$ and untagged $\bar{B}_s$, $B_s \to \phi(\to K^+K^-)\bar{\ell}\ell$ decays at NLO*, *JHEP* **07** (2008) 106 [arXiv:0805.2525] [INSPIRE].

[25] W. Altmannshofer et al., *Symmetries and asymmetries of $B \to K^*\mu^+\mu^-$ decays in the Standard Model and beyond*, *JHEP* **01** (2009) 019 [arXiv:0811.1214] [INSPIRE].

[26] A. Bharucha, D.M. Straub and R. Zwicky, *$B \to V\ell^+\ell^-$ in the Standard Model from light-cone sum rules*, *JHEP* **08** (2016) 098 [arXiv:1503.05534] [INSPIRE].

[27] UTfit collaboration, *The unitarity triangle fit in the standard model and hadronic parameters from lattice QCD: a reappraisal after the measurements of Δm_s and $BR(B \to \tau\nu_t au)$*, *JHEP* **10** (2006) 081 [hep-ph/0606167] [INSPIRE].

[28] D. van Dyk et al., *EOS — A HEP Program for Flavour Observables*, (2018).

[29] S. Descotes-Genon, J. Matias and J. Virto, *Understanding the $B \to K^*\mu^+\mu^-$ anomaly*, *Phys. Rev.* **D 88** (2013) 074002 [arXiv:1307.5683] [INSPIRE].

[30] W. Altmannshofer and D.M. Straub, *New physics in $B \to K^*\mu\mu$?*, *Eur. Phys. J.* **C 73** (2013) 2646 [arXiv:1308.1501] [INSPIRE].

[31] F. Beaujean, C. Bobeth and D. van Dyk, *Comprehensive Bayesian analysis of rare (semi)leptonic and radiative B decays*, *Eur. Phys. J.* **C 74** (2014) 2897 [*Erratum ibid.* **C 74** (2014) 3179] [arXiv:1310.2478] [INSPIRE].

[32] T. Hurth and F. Mahmoudi, *On the LHCb anomaly in $B \to K^*\ell^+\ell^-$*, *JHEP* **04** (2014) 097 [arXiv:1312.5267] [INSPIRE].

[33] F. Beaujean, C. Bobeth and S. Jahn, *Constraints on tensor and scalar couplings from $B \to K\bar{\mu}\mu$ and $B_s \to \bar{\mu}\mu$*, *Eur. Phys. J.* **C 75** (2015) 456 [arXiv:1508.01526] [INSPIRE].

JHEP10(2019)236

[34] A. Paul and D.M. Straub, *Constraints on new physics from radiative B decays*, *JHEP* **04** (2017) 027 [arXiv:1608.02556] [INSPIRE].

[35] S. Jäger, M. Kirk, A. Lenz and K. Leslie, *Charming new physics in rare B-decays and mixing?*, *Phys. Rev.* **D 97** (2018) 015021 [arXiv:1701.09183] [INSPIRE].

[36] A. Mauri, N. Serra and R. Silva Coutinho, *Towards establishing lepton flavour universality violation in $B \to K^* \ell\ell$ decays*, *Phys. Rev.* **D 99** (2019) 013007 [arXiv:1805.06401]

[37] LHCb collaboration, *Measurements of the S-wave fraction in $B^0 \to K^+\pi^-\mu^+\mu^-$ decays and the $B^0 \to K^*(892)^0\mu^+\mu^-$ differential branching fraction*, *JHEP* **11** (2016) 047 [*Erratum ibid.* **04** (2017) 142] [arXiv:1606.04731] [INSPIRE].

[38] J. Matias, *On the S-wave pollution of $B \to K * \ell^+\ell^-$ observables*, *Phys. Rev.* **D 86** (2012) 094024 [arXiv:1209.1525] [INSPIRE].

[39] T. Blake, U. Egede and A. Shires, *The effect of S-wave interference on the $B^0 \to K^{*0}\ell^+\ell^-$ angular observables*, *JHEP* **03** (2013) 027 [arXiv:1210.5279] [INSPIRE].

[40] D. Becirevic and A. Tayduganov, *Impact of $B \to K_0^*\ell^+\ell^-$ on the new physics search in $B \to K^*\ell^+\ell^-$ decay*, *Nucl. Phys.* **B 868** (2013) 368 [arXiv:1207.4004] [INSPIRE].

[41] D. Aston et al., *A study of $K^-\pi^+$ scattering in the reaction $K^-p \to K^-\pi^+n$ at 11 GeV/c*, *Nucl. Phys.* **B 296** (1988) 493 [INSPIRE].

[42] J.A. Bailey et al., *$B \to Kl^+l^-$ decay form factors from three-flavor lattice QCD*, *Phys. Rev.* **D 93** (2016) 025026 [arXiv:1509.06235] [INSPIRE].

JHEP10(2019)236